FT-IR AND RAMAN SPECTROSCOPY OF ZnO AND MgO CONTAINING GLASSES IN THE $B_2O_3/Na_2O/CaO/P_2O_5$ SYSTEM

Tina Tasheva, Gabriela Valova

University of Chemical Technology and Metallurgy
Department of Silicate Technology
8 Kliment Ohridski Blvd., Sofia 1797, Bulgaria
E-mail: tina.tasheva@uctm.edu

Received 14 September 2023
Accepted 16 December 2023
DOI: 10.59957/jctm.v59.i6.2024.14

ABSTRACT

Glasses with compositions $46.1B_2O_3$-$24.4Na_2O$-$26.9CaO$.$2.6P_2O_5$, $xZnO/MgO$-$22.0B_2O_3$-$(24.4-x)Na_2O$-$27CaO$-$2.5P_2O_5$ (x = 2.5, 3 mol%) and $1.5ZnO$-$1.5MgO$-$22.0B_2O_3$-$21.5.Na_2O$-$27CaO$-$2.5P_2O_5$ were melted by melt quenching technique. The densities of the glasses were measured by the Archimedes principle, using an analytical scale. Glasses possess densities in the 2.538 to 2.623 g cm^{-1} range. The short-range order was also discussed from the molar volume Vm, cm^3 mol^{-1}, and oxygen packing density point of view. The molar volume of the glasses varies between 26.566 - 27.420 cm^3 mol^{-1} and the oxygen packing density is between 73.669 to 76.262 mol cm^{-3}. The Furie transform infrared spectroscopy and Raman spectroscopy were performed to study the main structural units constituting the structure of the samples. The main structural units were found to be BO_3 and BO_4 probably connected in pentaborate and triborate structural units. The influence of the ZnO and MgO on the structure and chemical bonding of the glasses was discussed.

Keywords: Borate glasses, FT-IR spectroscopy, Raman spectroscopy.

INTRODUCTION

The successful advancement of reconstructive surgery, orthopaedics, dentistry, and various other medical fields heavily relies on progress in medical materials science. The discovery and development of new materials require the integration of essential mechanical and chemical properties with biocompatibility or biological activity within living tissue. Ceramic materials stand out due to their durability and resistance in extreme conditions, unlike other materials, and remain stable without dissolving or losing properties when used in the human body. Bioceramics, a significant and diverse category of biomaterials, are often indispensable for the temporary or permanent replacement of elements within the human support system. These ceramic materials are commonly used to repair or reconstruct diseased or damaged components of the musculoskeletal system. Among them, bioactive glasses and glass-ceramics have garnered significant attention for their promising applications.

Bioactive silicate glasses have been intensively studied since Bioglass® development. Bioglass is a sodium-calcium-phosphosilicate (Na_2O-CaO-P_2O_5-SiO_2) glass that reacts in the physiological environment. When implanted, the glass breaks down slowly and the dissolution products stimulate the progenitor cells to differentiate along the bone cell (osteoblast) pathway by stimulating genes associated with osteoblast differentiation. The glass binds to the existing bone (osseointegration) and promotes the growth of new bone on its surface (osteoconductive). Bone bonding is due to the formation of a layer of calcium phosphate (hydroxycarbonate apatite, HCA) on the glass surface, which occurs in the first few hours after implantation. The HCA layer has a similar composition to natural bone minerals. Collagen fibrils from the host bone are thought to interact through cellular processes with the fine (nano)

scale topography. Silicate glasses show high potential in biomedicine applications; however, they have a low solubility rate, which limits their compatibility with biological tissues [1]. As an alternative, borate compounds, which are also glass-forming, are being studied currently. Borate glasses are more bioactive than silicates due to their higher HA conversion rate, low chemical durability, and fast dissolution rates when in contact with a biological fluid [1]. Furthermore, boron is an essential element for bone growth and promotes new bone formation by enhancing osteoblast proliferation [2]. Borate glass scaffolds also facilitate vascularization by inducing angiogenesis along with the formation of new bone at the site of the defective bone [3]. In addition, H_3BO_3 formed from the breakdown of borate glasses acts as an effective antiseptic, aiding the wound healing process. Thus, borate glass scaffolds can be considered suitable for both bone and soft tissue engineering applications [4 , 5]. However, they degrade rapidly and a sudden increase in ion concentration (BO_3^{3-}) can be cytotoxic [6].

The present study focuses on the structural changes of borate glasses within the B_2O_3-Na_2O-CaO-P_2O_5 system with ZnO and MgO addition.

EXPERIMENTAL

Glasses with compositions 46.1B_2O_3-24.4Na_2O-26.9CaO.2.6P_2O_5, xZnO/MgO-22.0B_2O_3-(24.4-x) Na_2O-27CaO-2.5P_2O_5 (x = 2.5, 3 mol%) and 1.5ZnO-1.5MgO-22.0B_2O_3-21.5.Na_2O-27CaO-2.5P_2O_5 are melted by melt quenching technique. The compositions of the obtained glasses are given in Table 1. Reagent grade commercial powders of B_2O_3, Na_2CO_3, CaO, ZnO, MgO, and H_3PO_4 were mixed and melted in a porcelain crucibles at 650°C for 20 min and 950°C for 20 min in electric furnace. The melts were poured onto an alumina plate and pressed to a thickness of 1~2 mm by another copper plate. The amorphous nature of the samples was identified using X-Ray diffractometer Bruker advansed X-Ray, Cu-Kα radiation in the range of 5.3 - 80 2θ with constant step 0.02, 0.1 sec/step. The densities of the glasses were measured by the Archimedes principle, using an analytical scale Mettler Toledo New Classic ME 104 equipped with density determination kit for solids using distilled water as the immersion liquid. For each glass composition, density was measured at least ten times of at least three different samples. The short-range order was also discussed from the molar volume Vm, $cm^3 mol^{-1}$, and oxygen packing density point of view. The spectra of the glasses were recorded in the 2000 - 400 cm^{-1} range by using FT-IR spectrometer Varian 600-IR. The samples for these measurements were prepared as KBr discs. The precision of the absorption maxima was 3 cm^{-1}. Raman Renishaw inVia microscope with Leica DM2700 M; Analysis' conditions: laser: 532 nm, integration time - 10 seconds, laser power - 5mW, 3 accumulations.

RESULTS AND DISCUSSION

The results of the X-ray powder diffraction of the samples are presented in Fig. 1. No sharp peak is observed which indicates absence of a crystalline nature. The curve shows only broad diffuse scattering at about 20 - 30 2θ angles which is characteristic of long range disorder. This refers to the amorphous nature of the samples investigated.

Table 1. Sample notation and compositions of the glasses, mol %.

	B_2O_3	Na_2O	CaO	ZnO	MgO	P_2O_5
G1.0	46.1	24.4	26.9	-	-	2.6
G1.1	46	22	27	2.5	-	2.5
G1.2	46	21.5	27	3	-	2.5
G1.3	46	21.5	27	1.5	1.5	2.5
G1.4	46	21.5	27	-	3	2.5
G1.5	46	22	27	-	2.5	2.5

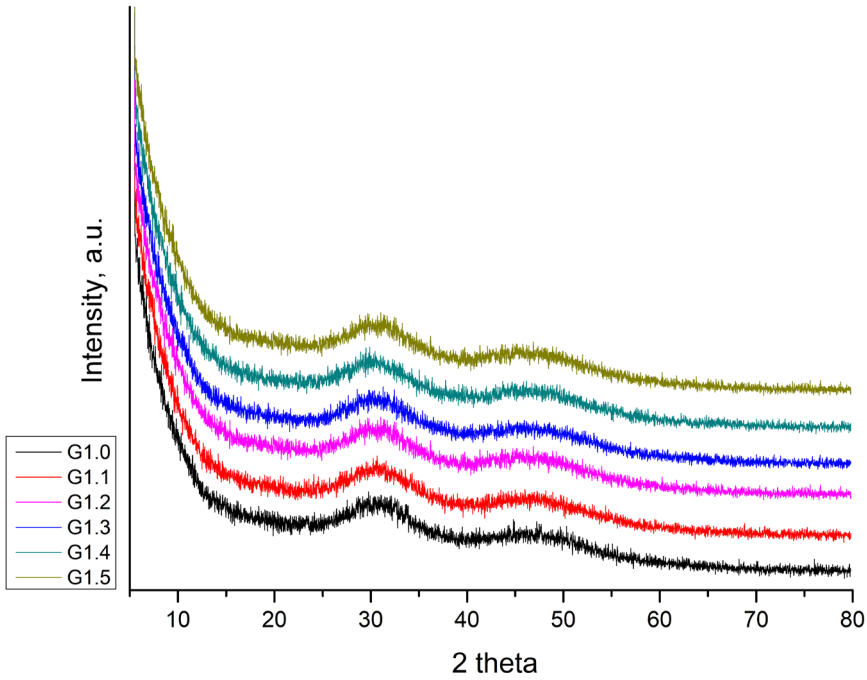

Fig. 1. X-ray patterns of the glasses.

The results of the density measurements are presented in Table 2. Based on the measured density, the molar volume, Vm, was calculated using the following equation:

$$V_m = \frac{M_i}{d_i} = \frac{\sum x_i M_i}{d_i}, \text{ cm}^3 \text{ mol}^{-1} \quad (1)$$

where: M_i is the molar mass of the glass, d_i is the density, x_i is the molar fraction of each component i, of the corresponding glass.

The oxygen packet density, OPD, of the glasses was determined by:

$$OPD = 1000.N_O^{2-}.\frac{d_i}{M_i}, \text{ mol cm}^{-3} \quad (2)$$

where N_O^{2-} is the number of oxygens for one molecule of glass.

The results obtained for the molar volume Vm, and the oxygen packet density OPD, are presented in Table 2. The relationship between density, molar volume and oxygen packet density as a function of composition was traced. The results are shown in Figs. 2 - 4. It is noteworthy to mention that the addition of ZnO and MgO to the system leads to a decrease in the density of the glasses compared to the base composition, except composition G1.1 containing 2.5 mol % ZnO. The addition of 1.5 mol% of both ZnO and MgO leads to a decrease in density, an increase in molar volume, and a decrease in oxygen packing density. Glasses containing 2.5 mol % MgO have a lower density, higher molar volume and lower oxygen packing density compared to these containing the same amount of ZnO. Glass with 3 mol% MgO has a slightly higher density, smaller molar volume, and higher oxygen packet density compared to

Table 2. Sample notations, density, d, molar mass, M, molar volume, Vm, and oxygen packing density.

	d, g cm^{-3}	M, g mol^{-1}	Vm, cm^3 mol^{-1}	OPD, mol cm^{-3}
G1.0	2.623	69.684	26.566	76.262
G1.1	2.630	70.254	26.712	75.620
G1.2	2.568	70.415	27.420	73.669
G1.3	2.552	69.606	27.275	74.060
G1.4	2.589	68.798	26.573	76.017
G1.5	2.538	68.906	27.150	74.402

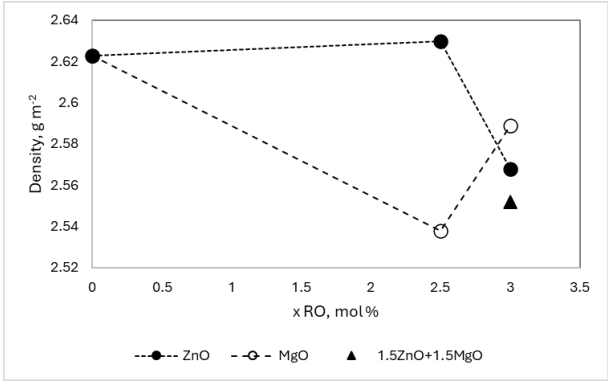

Fig. 2. Density as a function of the composition.

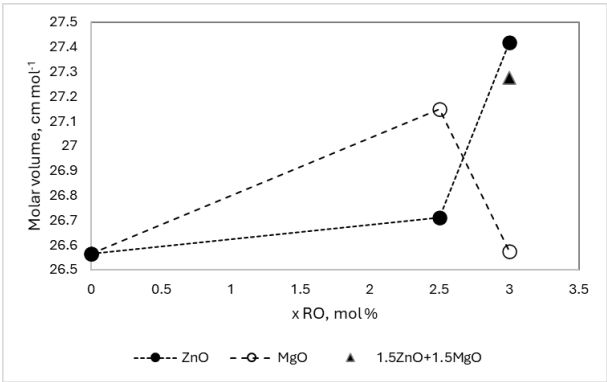

Fig. 3. Molar volume as a function of the composition.

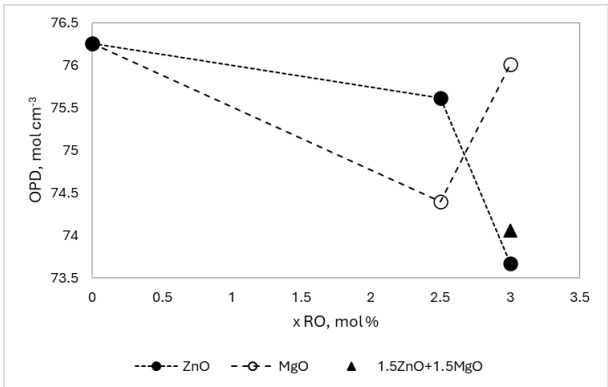

Fig. 4. Oxygen packing density as a function of the composition.

that containing ZnO. The molar volume, Vm, reflects free space and the formation of non-bridge oxygens (NBOs) in the glass structure, while the oxygen packet density (OPD) is sensitive to the cross-linkage of the structure. An increase in molar volume implies an increase in free space and the formation of non-bridge oxygens (NBOs) in the glass structure, and an increase in oxygen packet density is due to the formation of a stronger and highly cross-linked network resulting in a more tightly packed amorphous network.

To elucidate the nature of chemical bonding in the $B_2O_3/Na_2O/CaO/P_2O_5$, $ZnO/B_2O_3/Na_2O/CaO/P_2O_5$, $MgO/B_2O_3/Na_2O/CaO/P_2O_5$ and $ZnO/MgO/B_2O_3/Na_2O/CaO/P_2O_5$ IR-spectra of the glasses were recorded. The spectra are presented in Fig. 5. The analysis of the spectra was made based on the characteristic vibrations of metal-oxygen units found in various binary and triple crystalline and amorphous materials with similar composition. The spectra for glass without ZnO and/or MgO (G1.0) are characterized by bands at 562 cm^{-1}, 712 cm^{-1}, 938 cm^{-1}, 1007 cm^{-1}, 1193 cm^{-1} and 1416 cm^{-1}. The addition of ZnO and MgO even in small quantities lead to shift in some of the bands: in the high frequency region the band at about 1415 - 1395 cm^{-1}, the band at 1195 - 1251 cm^{-1} and the region between 940 and 1021 cm^{-1}. The region between 940 and 1021 cm^{-1} in the spectra of the glass with 1.5 mol % ZnO and MgO is different than the spectra of the other glasses. Instead of broad band with two well defined peaks the spectrum is characterized with only one peak at 986 cm^{-1}. The band at around 1200 cm^{-1} in this glass is significantly shifted-up to 1250 cm^{-1}. These changes suggest structural changes.

In general, the vibrational spectra of borates have a complicated character and their unambiguous interpretation is difficult due to the proximity in the oscillatory frequencies of the individual structural groups. The isolated BO_3 group is a flat trigonal structural unit with a D_{3h} point symmetry group. Characteristic frequencies corresponding to this group in the borate spectra are $\nu_s(A1)$ at 940 - 925 cm^{-1}, $\delta(A2)$ at 765 - 725 cm^{-1}, $\nu_d^{as}(E)$ at 1310 - 1000 cm^{-1}, and $\delta_d(E)$ at 680 - 590 cm^{-1}. Various studies have shown that the range between 1550 - 1150 cm^{-1} is the most characteristic range for demonstrating BO_3 groups [7 , 8]. With high symmetry of BO_3, the first vibration is not active in the IR spectrum, and the degenerate stretching $\nu_d^{as}(E)$ and bending $\delta_d(E)$ vibrations have a singlet structure. When the symmetrical decreases, the symmetric valence vibrations become active in the spectrum, and the bands associated with the degenerate vibrations split into a doublet. The IR spectra of borates containing tetrahedral BO_4 group are characterized by intense bands in the region of 1150 - 850 cm^{-1}. Vitreous B_2O_3, which is made up of boroxol rings and independent BO_3 groups,

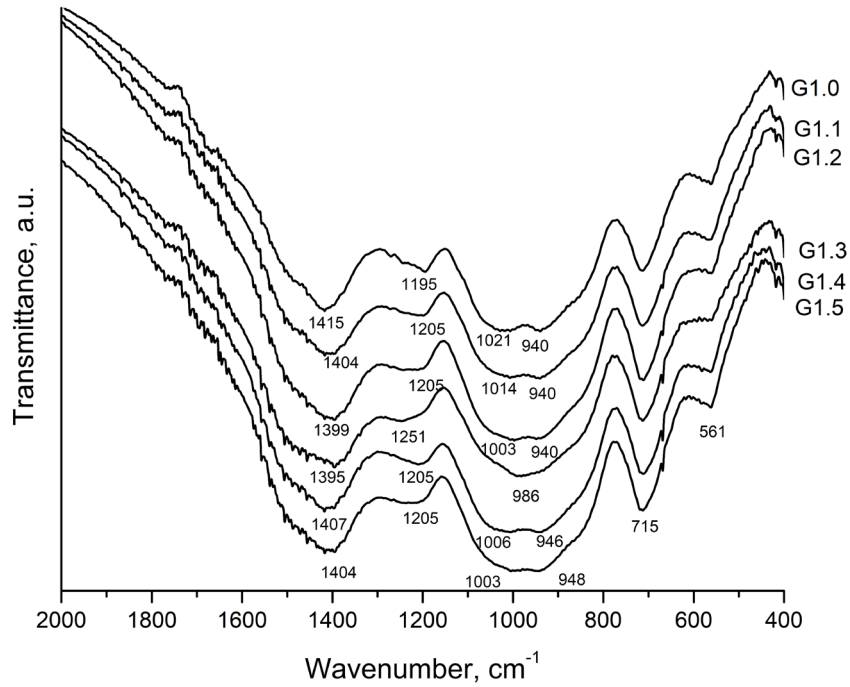

Fig. 5. FT-IR spectra of the glasses.

has no bands in the IR spectrum in this region, unlike the Raman spectrum, where evidence of the presence of boroxol rings is the appearance of a band at about 800 cm^{-1} [7 - 11].

G.J. Mohini et al. studies bioactive multi component glasses of the composition of 27.4 B_2O_3-6.4SiO_2-2.5P_2O_5-25.5Na_2O-(38.2-x)CaO:xAl_2O_3 (x = 0 and 3.2 mol %) by means of FT-IR spectroscopy [12]. They found that the structure of the glass with composition 27.4B_2O_3-6.4SiO_2-2.5P_2O_5-25.5Na_2O-38.2CaO is built up of BO_3 and BO_4 units. The band at 1390 cm^{-1} they assign to the B-O stretching vibrations od BO_3 units, the band at 1224 cm^{-1} to the PO^{2-} asymmetric groups, P=O stretching, 1026 cm^{-1} to ν_3-Si-O stretching and BO_4 units, 938 cm^{-1} to PO_4^{3-} groups, 729 cm^{-1} to B-O-B, 556 cm^{-1} to ν_4-P-O bending mode and the band at 487 cm^{-1}.

According to the data above, the band at high frequency region (1395 - 1415 cm^{-1}) can be assign to the B-O degenerate stretching vibration $\nu_d^{as}(E)$ of trigonal BO_3 unit, and the band at 561 cm^{-1} to the degenerate bending vibration $\delta_d(E)$ of BO_3 units. The absence of peak around 800 cm^{-1} in our spectra indicates that borate network does not contain any boroxol rings. The band about 1200 cm^{-1} could be assign to the vibration of pyroborate units $B_2O_5^{4-}$, while the band at 1251 cm^{-1} could be due to the vibrations of triborate groups. The same region is characteristic for the P=O stretching vibrations of PO^{2-} asymmetric groups. The band at 715 cm^{-1} is assigned to the B-O-B linkages between the pyroborate groups. The bands at 940 cm^{-1} and 1021 cm^{-1} could be due to the B-O stretching vibrations of BO_4 tetrahedra in pentaborate units, while the band at 986 cm^{-1} in the spectra of glass with 1.5 mol% MgO and ZnO corresponds to the vibrations of triborate and diborate groups. In summary, the main structural units of the glasses are BO_3 and BO_4 connected in pentaborate and pyroborate groups for all compositions while the glass with both 1.5 mol % ZnO and 1.5 mol % MgO are characterized by triborate or diborate units. Thus, the addition of both oxides leads to BO_3 to BO_4 transformation.

In Fig. 6 the Raman spectra of the glasses are presented. In the Raman spectra can be seen four main bands: at 552 cm^{-1}, 771 cm^{-1}, 950 cm^{-1}, and 1490 cm^{-1}.

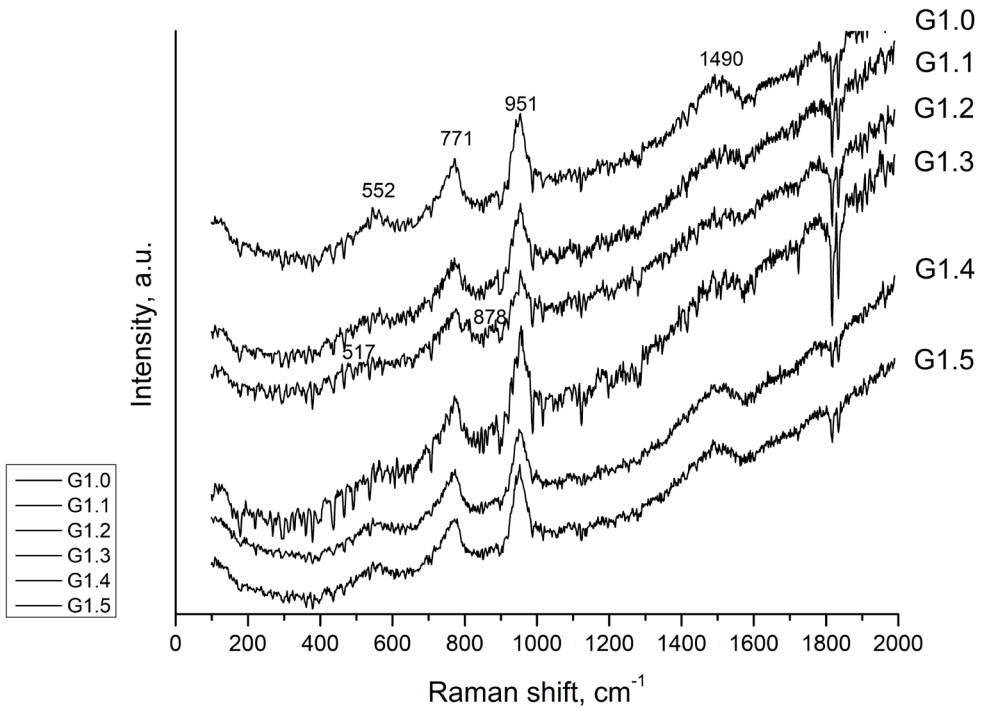

Fig. 6. Raman spectra of the glasses.

In the spectra of glasses G1.3 and G1.4 the band at 552 cm^{-1} is missing but small band at about 517 cm^{-1} appears and well as a band at 878 cm^{-1}.

Raman spectroscopy provided the strongest early evidence for the existence of the boroxol ring [13]. The planar boroxol rings are readily identifiable in Raman spectroscopy by a strong, highly symmetric band at 805 cm^{-1}. The band arises from the symmetric stretch of the bridging oxygen atoms of the ring breathing mode and has been shown to be independent of the boron atoms by investigation using isotopic ^{10}B ^{11}B substitution. Because of its sharpness and strong intensity, this characteristic band is visible in the Raman spectra of many modified borate glasses. Aside from the ring breathing of the boroxol ring, other features observable in the Raman spectra of vitreous B_2O_3 are the symmetric stretch of the oxygen bridging two boroxol rings (~460 cm^{-1}) and less so the bending modes of the loose BO, triangles between 620 and 760 cm^{-1} as well as B-O stretching modes above 1200 cm^{-1} [13].

S. Aqdim et al. studied physico-chemical properties, structure and bioactivity of glasses in with composition (14-x) Na_2O-(54+*x*) B_2O_3- 8MgO-22CaO-2P_2O_5 with *x* = 0, 4, 7, 10, 14 mol % [14]. According to their results three characteristic bands (υ_1-υ_3) of the tetrahedrally coordinated borate species appear at υ_1= 760 cm^{-1}, υ_2= 850 cm^{-1} and υ_3=920 cm^{-1}. The υ_1 and υ_3 modes represent the vibrations of the pentaborate groups which is an arrangement containing one or two B$Ø_4$-tetrahedral (Ø bridging oxygen) and υ_2 can be attributed to any tetrahedrally coordinated borate groups [14]. At high frequency (> 1000 cm^{-1}) five characteristic bands (υ_4-υ8) of borate units together with phosphates are represented with the following modes υ_4= 1127 cm^{-1}, υ_5= 1224 cm^{-1}, υ_6 =1306 cm^{-1}, υ_7 =1378 cm^{-1}, υ_8 =1469 cm^{-1}. Their attribution is based on literature and the evolution of the band parameters, where υ_4 and υ_5 are attributed to $\upsilon_s(PO_2)$ and $\upsilon_{as}(PO_2)$ respectively, υ_6 can be assigned to the pyroborate groups, whereas υ_7 and υ_8 corresponded to BO_2O^- triangle either linked to BO_4^- or to another triangular unit respectively [14].

Based on the mentioned above, we cannot expect the presence of any boroxol rings in the structure of the glasses in this study. The band at 771 cm^{-1} could be

explained by the bending vibrations δ(A2) of trigonal BO_3 unit and the stretching vibration of tetragonal BO_4 unit of pyroborate unit, the band at 951 cm^{-1} is also related by the vibrations of pentaborate units. The band at 850 cm^{-1} could be attributed to any tetrahedrally coordinated borate groups, and the band at 1490 cm^{-1} corresponded to BO_2O^- triangle either linked to BO_4^- or to another triangular unit.

CONCLUSIONS

Glasses with composition $46.1B_2O_3$-$24.4Na_2O$-$26.9CaO.2.6P_2O_5$, $xZnO/MgO$-$22.0B_2O_3$-$(24.4-x)$ Na_2O-$27CaO$-$2.5P_2O_5$ (x = 2.5 and 3 mol%) and 1.5ZnO-1.5MgO-$22.0B_2O_3$-$21.5.Na_2O$-$27CaO$-$2.5P_2O_5$ were melted by melt-quenching technique. The densities of the glasses were measured and molar volume and the oxygen packing density were calculated. The addition of 1.5 mol % ZnO and MgO altogether in the glasses cause a change in the structure. The density of the glasses decrease, the molar volume increases and the oxygen packing density decreases, i.e the free space and the formation of non-bridge oxygens NBOs increases and the network is less cross-linked compared to the compositions with only ZnO and MgO or without any ZnO or MgO. The main structural units were found to be BO_3 and BO_4 connected by B-O-B linkages in pentaborate and pyroborate structural units except for the glasses with mutual presence of ZnO and MgO where triborate structural units are possibly formed.

Acknowledgements

This research is supported by the Bulgarian National Science Fund, Competition for financial support for projects of junior basic researchers and postdocs-2022 under grant KП-06-M69/6 and BG-RRP-2.004-0002-C01, project name: BiOrgaMCT, Procedure BG-RRP-2.004 „Establishing of a network of research higher education institutions in Bulgaria", funded by Bulgarian National Recovery and Resilience Plan. The authors would like to express their gratitute to prof. Daniela Kovacheva and her group for the XRD measurements, IGIC-BAS.

REFERENCES

1. G. Lopes da Silva, I.F. Rodrigues, S.S.S. Pereira, G.M.G. Fontoura, A.S. Reis, F. Pedrochi, A. Steimacher, Bioactive antibacterial borate glass and glass-ceramics, J. Non-Cryst. Solids, 595, 2022, 121829.
2. P. Balasubramanian, T. Büttner, V.M. Pacheco, A.R. Boccaccini, Boron-containing bioactive glasses in bone and soft tissue engineering, J. Eur. Ceram. Soc., 38, 2018, 855-869.
3. L. Bi, B. Zobell, X. Liu, M.N. Rahaman, L.F. Bonewald, Healing of critical-size segmental defects in rat femora using strong porous bioactive glass scaffolds, Mater. Sci. Eng. C., 42, 2014, 816-824.
4. X. Liu, M.N. Rahaman, D.E. Day, Conversion of melt-derived microfibrous borate (13-93B3) and silicate (45S5) bioactive glass in a simulated body fluid, J. Mater. Sci. Mater. Med., 24, 2013, 583-595.
5. Y. Lin, R.F. Brown, S.B. Jung, D.E. Day, Angiogenic effects of borate glass microfibers in a rodent model, J. Biomed. Mater. Res. - Part A., 102, 2014, 4491-4499.
6. M.N. Rahaman, Bioactive ceramics and glasses for tissue engineering, In book: Tissue Engineering Using Ceramics and Polymers, 2014, 67-114.
7. B. Topper, E.M. Tsekrekas, L. Greiner, R.E. Youngman, E.I. Kamitsos, D. Möncke, The dual role of bismuth in Li_2O-Bi_2O_3-B_2O_3 glasses along the orthoborate join, J. Am. Ceram. Soc., 105, 2022, 7302-7320.
8. V. Dimitrov, Y. Dimitriev, Structural analysis (spectral methods), UCTM Publishing house, Sofia, 2009, (in Bulgarian).
9. J.A. Kapoutsis, E.I. Kamitsos, G.D. Chryssikos, A structural study of silver borate glasses by infrared reflectance and Raman spectroscopies, Borate glasses, crystals & melts, Proc. Second Int. Conf. on Borates Glasses, Crystals and melts, Edited by A.C. Whright, S.A. Feller, A.C. Hannon, The society of Glass Technology, Sheffield, 1997, 303.
10. C. Gautam, A.K. Yadav, A.K. Singh, Review Article: A Review on Infrared Spectroscopy of Borate Glasses with Effects of Different Additives, Int. Scholarly Res. Network, ISRN Ceramics, 2012, Article ID 428497. doi:10.5402/2012/428497
11. AA.Ali, Y.S. Rammah, R.El-Mallawany, D. Souri, FTIR and UV spectra of pentaternary borate glasses, Measurement 105, 2017, 72-77.
12. G.J. Mohini, N. Krishnamacharyulu, G.S. Baskaran, P.V. Rao, N. Veeraiah, Studies of influence of aluminium ions on the bioactivity of B_2O_3-SiO_2-P_2O_5-

Na_2O-CaO glass system by means of spectroscopic studies, Appl. Surf. Sci., 287, 2013, 46-53.
13. B. Topper, D. Moncke, Structure and properties of borate glasses, Chapter 9, Biomat. Sci. Ser. 11, Phosphate and Borate Bioactive Glasses, Edited by Akiko Obata, Delia S. Brauer and Toshihiro Kasuga, The Royal Society of Chemistry 2022, Published by the Royal Society of Chemistry, www.rsc.org.
14. S. Aqdim, M. Naji, A. Chakir, A. El Bouari, Design, synthesis and structural roperties of borate glasses: Towards an alkali-free bioactive glasses, J. Non-Cryst. Solids, 597, 2022, 121876.